S. D. Bellows and T. W. Leishman, "Spherical harmonic expansions of high-resolution musical instrument directivities", Proc. Mtgs. Acoust. 35, 035005, 10.1121/2.0001274 (2018)

and may be found at https://doi.org/10.1121/2.0001274

Volume 35 http://acousticalsociety.org/

176th Meeting of Acoustical Society of America
2018 Acoustics Week in Canada
Victoria, Canada
5-9 November 2018

Musical Acoustics: Paper 4aMU5

Spherical harmonic expansions of high-resolution musical instrument directivities

Samuel David Bellows and Timothy Ward Leishman
Department of Physics and Astronomy, Brigham Young University, Provo, UT, 84602; samuel.bellows11@gmail.com; twleishman@byu.edu

Well-quantified directivity patterns of sound sources provide greater insights into their acoustical properties and the potential to simulate the propagation of their sounds in various settings. Moreover, clear descriptions of detailed spherically sampled directivities of highly complex and dynamic sound sources such as musical instruments have broad applications. Because spherical harmonics are a suitable basis set for representing functions on the sphere, this work reviews and compares methods for computing spherical harmonic expansion coefficients. It further presents distinct quadrature methods applicable to the five-degree polar and azimuthal sampling distribution commonly used in directivity measurements, and analysis regarding convergence and accuracy of the expansions. Finally, it presents selected results of spherical harmonic expansions of musical instruments.

Published by the Acoustical Society of America

 https://doi.org/10.1121/2.0001274

1. INTRODUCTION

Directivity measurements of sound sources are useful for a variety of applications, including spatial audio, architectural acoustics prediction and modeling, and helping researchers to understand the radiation characteristics of the sources themselves. While information on the directivities of loudspeakers and other transducers is widely available, directivities of live sources, such as musical instruments and speech, have received less attention due to the difficulties in performing reliable and high-resolution measurements. Once directivities are measured, spherical harmonic expansions are also useful in a variety of applications. This paper explores various techniques for computing spherical harmonic coefficients as well as presenting new methods applicable to the sampling scheme used for this work. It also compares the effectiveness and accuracy of the different techniques and presents selected results of the spherical harmonic expansions of measured high-resolution musical instrument directivities.

2. DIRECTIVITY MEASUREMENTS

The directivities of 16 musical instruments were measured using a multi-capture transfer-function technique as outlined in Ref. 1. The measurement apparatus utilized a fixed microphone arc with 5° polar angle increments along with a rotatable chair as shown in Fig. 1. The seated musician repeated a chromatic scale over the full range of the instrument, for each of 72 azimuthal rotations in 5° increments. The entire sphere was thus sampled with 5° polar and 5° azimuthal resolution, consistent with published AES standards on loudspeaker directivity measurements.[2] Because of inevitable changes in playing style, loudness, timbre, etc., due to human error repetition errors, a microphone was affixed in the near field of the musician's rotating frame to serve as the reference microphone in computing a frequency response function (FRF) between the reference and array microphone signals. Figure 2 illustrates the effectiveness of the FRF technique in compensating for the differences in playing between rotations. Figure 2a shows the uncalibrated autospectral balloon measured by the array microphones, with vertical banding apparent as an artifact of playing differences between rotations. Figure 2b shows the relatively calibrated FRF-based balloon, which compensates for these differences by using the near field reference microphone signal. A detailed description of the transfer-function technique, its effectiveness, and its limitations is beyond the scope of this work, but more information can be found in Ref. 1.

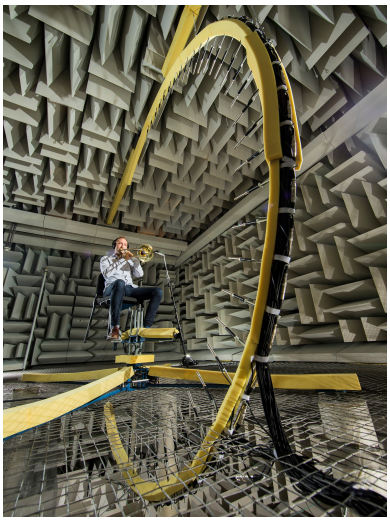

Figure 1: Microphone array used for measuring directivities of musical instruments and speech.

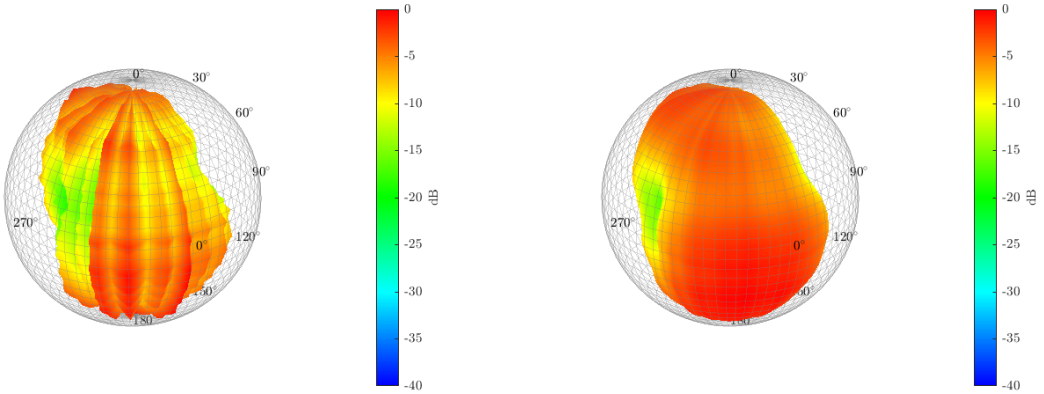

(a) The autospectral balloon. *(b) The frequency response balloon.*

Figure 2: Flute Directivity at 311 Hz (E♭ 4).

3. SPHERICAL HARMONIC REPRESENTATION OF FUNCTIONS

The spherical harmonics are useful for representing functions on the sphere and are solutions to the Helmholtz equation in spherical coordinates. Thus, they can be employed for various applications, such as acoustical holography, interpolation of functions and directivities, and estimating pressure in the far-field.[3] The normalized spherical harmonics $\{Y_n^m\}_{n\in\mathbb{N}_0,|m|\leq n}$ of degree n and order m, are defined as

$$Y_n^m(\theta,\phi) = \sqrt{\frac{2n+1}{4\pi}\frac{(n-m)!}{(n+m)!}}P_n^m(\theta,\phi)e^{im\phi}, \tag{1}$$

where θ and ϕ are the polar and azimuthal angles, respectively, and form a complete orthogonal basis for $L^2(\mathcal{S}^2)$, the space of Lebesgue square-integrable functions on the sphere $\mathcal{S}^2$. Thus, any function $f \in L^2(\mathcal{S}^2)$ may be represented as a linear combination of spherical harmonics

$$f = \sum_{n=0}^{\infty}\sum_{m=-n}^{n} a_n^m Y_n^m, \tag{2}$$

where a_n^m are the expansion coefficients. The coefficients are determined by the inner product

$$a_n^m = \langle f, Y_n^m \rangle, \tag{3}$$

which is defined as

$$\langle f, g\rangle = \int_0^{2\pi}\int_0^{\pi} f(\theta,\phi)g^*(\theta,\phi)\sin\theta d\theta d\phi, \tag{4}$$

the * denoting complex conjugation. The inner product induces the norm on $L^2(\mathcal{S}^2)$

$$||f||_{L^2} := \langle f, f\rangle^{1/2}. \tag{5}$$

In the respective sequence space, the norm is defined as

$$||a_n^m||_{\ell^2} = \left(\sum_{n=0}^{\infty}\sum_{m=-n}^{n}|a_n^m|^2\right)^{1/2}, \tag{6}$$

such that Parseval's relation is satisfied:

$$||f||_{L^2} = ||a_n^m||_{\ell^2}. \tag{7}$$

Both norms will be useful in studying the convergence of the spherical harmonic expansions.

4. COMPUTING SPHERICAL HARMONIC EXPANSION COEFFICIENTS

In practice, a function is sampled on the sphere at Q distinct points. From the measurements, the spherical harmonic coefficients can then be computed using a variety of techniques. This section reviews several traditional approaches and introduces new formulas. The techniques can be categorized into two general approaches: least-squares estimation and quadrature.

A. LEAST-SQUARES

The least-squares method is a powerful and portable technique applicable to a wide variety of sampling schemes with relative ease. It is based on the fact that the value of a function f at any sampling point (θ_q, ϕ_q) is a linear combination of the spherical harmonics evaluated at that sampling point:

$$f(\theta_q, \phi_q) = \sum_{n=0}^{\infty} \sum_{m=-n}^{n} a_n^m Y_n^m(\theta_q, \phi_q). \tag{8}$$

By truncating the infinite series to degree N, a system of Q equations with $(N+1)^2$ unknowns can be formulated:

$$\mathbf{f} = \mathbf{Y}\mathbf{a}, \tag{9}$$

where

$$\mathbf{f} = \begin{bmatrix} f(\theta_1, \phi_1) \\ f(\theta_2, \phi_2) \\ \vdots \\ f(\theta_q, \phi_q) \end{bmatrix}, \tag{10}$$

$$\mathbf{Y} = \begin{bmatrix} Y_0^0(\theta_1, \phi_1) & Y_1^{-1}(\theta_1, \phi_1) & \dots & Y_N^N(\theta_1, \phi_1) \\ Y_0^0(\theta_2, \phi_2) & Y_1^{-1}(\theta_2, \phi_2) & \dots & Y_N^N(\theta_2, \phi_2) \\ \vdots & \vdots & \ddots & \vdots \\ Y_0^0(\theta_q, \phi_q) & Y_1^{-1}(\theta_q, \phi_q) & \dots & Y_N^N(\theta_q, \phi_q) \end{bmatrix}, \tag{11}$$

and

$$\mathbf{a} = \begin{bmatrix} a_0^0 \\ a_1^{-1} \\ \vdots \\ a_N^N \end{bmatrix}. \tag{12}$$

In practice, N is usually chosen such that $(N+1)^2 < Q$ to avoid an ill-conditioned matrix $\mathbf{Y}$.[4] The least-squares solution to the over-determined system of equations is then given by

$$\mathbf{a} = \mathbf{Y}^{\dagger}\mathbf{f}, \tag{13}$$

where $\mathbf{Y}^{\dagger}$ is the pseudoinverse. One of the primary advantages of the least-squares approach is that it is readily applied to any sampling distribution; however, unlike quadrature rules, there is often no formulation on the degree of accuracy of the fit. Therefore, especially when sampling is space-limited, care must be taken to ensure the reliability of the fit. Furthermore, it should be noted that while the general rule-of-thumb that $(N+1)^2 < Q$ is useful for avoiding an ill-conditioned problem, a good condition number does not equate to the optimal convergence of the least-squares fit to the measured data. Since the choice of N is somewhat arbitrary, the least-squares approach requires some level of experimentation to determine the degree that provides the best convergence to the measured data. Nonetheless, when these considerations are taken into account, the least-squares approach is a straightforward and powerful technique for computing the spherical harmonic coefficients from measured data.

B. QUADRATURE

While the least-squares approach attempts to fit data to the spherical harmonic coefficients, the quadrature approach attempts to directly compute the coefficients by evaluating the inner product numerically. In general, a quadrature rule used to integrate a function $f(x)$ can be written as

$$\int_a^b f(x)dx = \sum_q w_q f(x_q) + E[f], \tag{14}$$

where w_q are the quadrature weights, typically unique to each x_q, the sampling nodes or points of collocation. Here $E[f]$ is an error function, which is dependent on the function f and the quadrature rule used. In many cases, $E[f] = 0$ up to some polynomial degree P. It is then said that the quadrature rule is exact to degree P. However, it should be understood that while such a quadrature rule can only integrate a function exactly up to degree P, it may be still be useful for integrating higher-degree functions, provided $E[f]$ remains sufficiently small. This principle will be illustrated later.

In using quadrature to calculate the spherical harmonic coefficients, one attempts to numerically integrate the inner product:

$$a_n^m = \sum_{q=1}^{Q} w_q f(\theta_q, \phi_q) Y_n^{m*}(\theta_q, \phi_q) + E[f] \tag{15}$$

Because $f(\theta_q, \phi_q)Y_n^{m*}(\theta_q, \phi_q)$ determines the highest degree of the integrated function, for a quadrature rule exact to degree P, the highest spherical harmonic coefficient that can be determined without error will be of degree $N = P/2$, as the product $Y_n^m(\theta_q, \phi_q)Y_n^{m*}(\theta_q, \phi_q)$ is a function of degree $2n$. Quadrature rules provide several notable benefits. To begin with, one can often use them to determine the exact values of the coefficients. Furthermore, as quadrature requires multiplication and addition, it does not require matrix inversion used by the least-squares method and can therefore be more stable. Another advantage is that having a method of integration on the sphere allows for computation of the norm in the function space as well as the sequence space, whereas the least-squares method only provides the norm in the sequence space. The capability of integrating functions over the sphere is also useful for other applications, such as calculating sound power. In similarity to the least-squares approximation, some level of experimentation is required to find the optimal highest degree N of the expansion. At first, one might conclude that the optimal degree would be the degree to which the scheme is exact; however, as will be shown later, the error functional $E[f]$ may remain small above the degree of exactness, meaning better convergence can be found using higher-degree terms. The difficulty with quadrature is that it requires a rule to be worked out for a given sampling scheme, whereas the least-squares method is easily portable from one sampling scheme to another. The following sections illustrate several quadrature rules that can be applied to numerical integration on the sphere. While some are unique to certain schemes, others are based on more general rules that can be applied to various sampling distributions.

i. Uniform Sampling

Equal-Area

A common approach to sampling is uniform or quasi-uniform sampling, in which sampling nodes are evenly distributed over the sphere, such as at the vertices of the platonic solids. In this case, the quadrature weights are given by dividing the total surface area of the sphere evenly among the sampling weights:[4]

$$w_q = \frac{4\pi}{Q}. \tag{16}$$

The result is that the spherical harmonic coefficients are given by

$$a_n^m = \sum_q w_q f(\theta_q, \phi_q) Y_n^{m*}(\theta_q, \phi_q). \tag{17}$$

When the sampling nodes have a quasi-uniform distribution, the uniform sampling weights can still provide a reasonable approximation.

ii. Gridded Sampling

While the uniform distribution of sampling nodes over the sphere has many advantages, it becomes infeasible for high-resolution sampling distributions. Often, rotating arrays or sources enable sampling with a rotate-and-repeat approach, such as that used in this study. In such case, the sphere is parameterized into a grid with fixed sampling nodes in one coordinate while the array or source is rotated through the other. This leads to two-dimensional gridded sampling, which allows a surface integral over the unit sphere to be evaluated in terms of the polar and azimuthal coordinates independently, that is

$$\int_0^{2\pi} \int_0^{\pi} f(\theta, \phi) \sin\theta d\theta d\phi \approx \sum_{u=1}^{U} \sum_{v=1}^{V} a_u b_v f(\theta_u, \phi_v), \tag{18}$$

where a_u are the sampling weights in the polar angle θ and b_v are the sampling weights in the azimuthal angle ϕ, such that $w_q = a_u b_v$. Often, the incremental azimuthal rotation angle $\Delta\phi$ is consistent across the entire measurement, such that

$$b_v = \frac{2\pi}{V}. \tag{19}$$

The following sections outline various quadrature rules applicable to the θ coordinate. It is assumed that the polar angle sampling has a uniform incremental angle $\Delta\theta$. Thus, Gauss-Legendre quadrature rules will not be considered. While the quadrature rules are applicable to different increments, it is assumed that $\Delta\theta = \Delta\phi = 5°$, the same as that used for this work as well as those commonly used for measuring loudspeaker directivities and architectural acoustics applications.[5] This is referred to herein as dual equi-angular sampling. It results in 37 samples with in θ and 72 samples in ϕ, leading to 2,522 unique sampling positions on the sphere.

Effective-Area

A simple approximation for a sampling scheme is to assign an effective area to each position, such as that described in the ISO standard for measuring sound power.[6] In the case of uniform sampling over the entire sphere, this approach yields exact quadrature rules; however, even for gridded sampling, in which the

nodes are not uniformly distributed on the sphere, the approach is still useful. For uniform sampling in the polar direction θ including the poles, the weights are:[7]

$$a_u = \begin{cases} 2\sin^2\frac{\Delta\theta}{4}, & \theta_u = 0, \pi \\ 2\sin\theta_u \sin\frac{\Delta\theta}{2}, & \theta_u \neq 0, \pi \end{cases}. \tag{20}$$

However, it was found empirically in the present work that modifying the weights at the pole to be $3/4^{th}$ their original value provided better results; however, this makes the quadrature rule inexact, even for degree $N = 0$. Nonetheless, as will be shown later, the approach is still quite accurate, surpassing the utility of several other rules.

Newton-Cotes

Newton-Cotes quadrature, which includes the trapezoidal and Simpson's rules, is based on constructing and integrating the Lagrange interpolating polynomial and requires evenly spaced nodes. While it is possible to construct quadrature rules accurate to an arbitrarily high degree using this method, they become more unstable at higher degrees. Thus, composite rules of lower degrees are typically used. For example, the composite Simpson's $3/8^{th}$ rule repeats the $3/8^{th}$ rule over m odd subintervals, such that the integral is approximated as[8]

$$\int_0^\pi f(\theta)\sin\theta d\theta \approx \frac{3\Delta\theta}{8}(f(\theta_1)\sin\theta_1 + 3f(\theta_2)\sin\theta_2 + 3f(\theta_3)\sin\theta_3 + 2f(\theta_4)\sin\theta_4 + ... + f(\theta_U)\sin\theta_U). \tag{21}$$

While this rule can exactly integrate only cubic polynomials on each subinterval, composite Simpson's rules are common and straightforward to use.

Equi-Angular

Equi-angular sampling consists of evenly spaced intervals in the polar angle θ with azimuthal sampling in twice as large of increments, i.e., $\Delta\phi = 2\Delta\theta$. The weights w_q for this sampling are given in Ref 9. However, noting that the azimuthal dependence of b_v and polar dependence a_u can be factored out of w_q, the sampling weights can be applied to dual equi-angular sampling by modifying the b_v component to adjust for twice the number of azimuthal samples. The polar weight a_u then becomes:

$$a_u = \frac{4}{U}\sin\theta_u \sum_{n=0}^{\frac{U}{2}-1} \frac{1}{2n+1}\sin((2n+1)\theta_u). \tag{22}$$

While both sampling schemes have samples at the poles, it is apparent that the corresponding weight $a_u = 0$, such that the values at the poles are not used. These weights are accurate for computing spherical harmonic expansions up to degree $N = 17$ for the 5° resolution sampling standard.

Chebyshev

Chebyshev integration uses Chebyshev polynomials as the interpolating function. When the nodes are equally spaced on the interval $[0, \pi]$ with respect to θ and include nodes at the poles, the general form of the weights are given by Mason and Handscomb as[10]

$$a_u = \sum_{j=0}^{N}{}'' \frac{c_j}{N} T_j(y_q), \tag{23}$$

where $y_q = \cos\frac{q\pi}{N}$, $T_j(x)$ are the Chebyshev polynomials, and $''$ indicates that the first and last terms in the summation are halved. To apply the quadrature rule to sampling on the sphere, the coefficients c_j must be determined; they are found by integration:

$$c_j = \int_{-1}^{1} w(x)T_j(x)dx = \int_0^{\pi} w(\cos\theta)\cos j\theta \sin\theta d\theta, \tag{24}$$

where $w(\cos\theta)$ is a weighting function (not to be confused with the discrete weights a_u). On the sphere, $w(\cos\theta) = 1$ and the coefficients become

$$c_j = \frac{1+\cos j\theta}{1-j^2}, \tag{25}$$

where the singularity at $j = 1$ is taken to be 0. The resulting weights a_u are beneficial because, unlike those proposed by Driscoll and Heally, they take advantage of samples at both poles, which are often used for the axis of principal radiation of a loudspeaker. They still have maximum accuracy up to $N = 17$ when used in the computation of spherical harmonic coefficients.

5. ACCURACY AND CONVERGENCE

The spherical harmonic expansions are useful in that they allow the original function f to be represented in terms of an orthogonal basis set, as shown in Eq. (2). However, in practice, numerical errors are caused due to insufficient sampling or spatial measurement noise, which introduce high-degree terms. In such cases, it is important to assess the accuracy of the expansion as well as the optimal degree N needed for convergence. For quadrature methods, this may or may not be the highest degree of exactness of the method. One measure of the error is to compute the point-wise RMSD between each discrete sampling position:

$$RMSD = \sqrt{\sum_{q=1}^{Q} w_q \left(f(\theta_q,\phi_q) - \tilde{f}(\theta_q,\phi_q)\right)^2}, \tag{26}$$

where $\tilde{f}$ is the function f approximated through the expansion coefficients and w_q weight the distribution of samples over the sphere evenly[7] (quadrature weights may be used, in which case the RMSD can be seen as approximating an integral over the sphere). For quadrature methods, the ability to perform integration over the sphere is useful in that one can approximate both the norm of the continuous function and the norm of the series representation. From Parseval's relation [Eq. (7)] the two should be equal, but due to numerical errors, they will not be. Yet, the convergence of the ℓ^2 norm to the L^2 norm is a good indicator of the convergence of the series expansion to the function, as will be shown in the following section.

6. COMPARISON OF METHODS

This section compares various quadrature methods by first integrating distinct spherical harmonic functions. It then illustrates the various techniques for computing the spherical harmonic coefficients applied to a unit cube. The examples follow the AES standard for 5° degree sampling. The methods analyzed include least-squares, effective area, composite Simpson's $3/8^{th}$ rule, equi-anglar, and Chebyshev.

Figure 3 shows the quadrature weights a_u plotted over the polar angle θ for the selected quadrature schemes. As evidenced in the figure, the composite Simpson's $3/8^{th}$ shows large undulations, which is typical for Newton-Cotes quadrature. The equi-angle quadrature scheme shows less variation, followed by the Chebyshev and finally the effective area, which has no undulations.

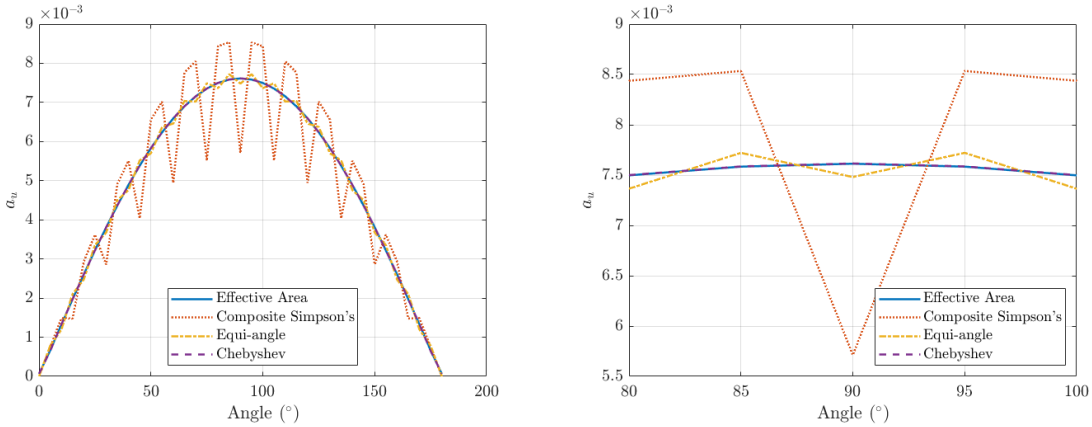

(a) Weights plotted between 0°and 180°. *(b) Weights plotted between 80°and 100°.*

Figure 3: Weights of various quadrature schemes plotted over θ.

Table 1 reports the value of the integral over the sphere of $Y_n^m Y_n^{m*}$ for various degrees n and order $m = 0$ (axisymmetric spherical harmonics). The table reveals important trends. First, while most of the schemes are exact to degree $N = 0$ (the modification of the effective area makes it inexact to any degree), only the equi-angular and Chebyshev weights are exact up to degree $N = 17$. Above this degree, the error from the Chebyshev quadrature is noticeably smaller than that of the equi-anglular quadrature. Interestingly, while the effective-area scheme was not exact even to degree $N = 0$, at high degrees, its accuracy of integration is still good.

Table 1: Integration of $Y_n^m Y_n^{m*}$

	Effective Area	Composite Simpson's 3/8th	Equi-anglular	Chebyshev
Y_0^0	0.9998	1.0000	1.0000	1.0000
Y_{10}^0	1.0007	1.0205	1.0000	1.0000
Y_{15}^0	1.0000	0.9777	1.0000	1.0000
Y_{17}^0	0.9992	0.9798	1.0000	1.0000
Y_{18}^0	0.9986	0.9803	0.9641	1.0000
Y_{20}^0	0.9970	0.9821	0.9616	0.9993
Y_{25}^0	0.9888	0.9324	0.9504	0.9922
Y_{30}^0	0.9615	0.9194	0.9199	0.9652
Y_{35}^0	0.3739	0.3292	0.3289	0.3772

The accuracy of various methods is emphasized in Fig. 4, which shows RMSD errors for spherical harmonic expansions performed for the unit cube. This was chosen due to its sharp edges, which induce high-degree terms and ensures that the discrete sampling scheme will always have some amount of spatial aliasing. For both Figs. 4a and 4b, the cube was sampled using 5° resolution and spherical harmonic coefficients were computed to various degrees. Figure 4a shows the RMSD between the spherical harmonic expansion evaluated at the sampled positions and the actual value at those positions. Fig. 4b shows the RMSD over a finer grid (2.5°resolution). Thus, Fig. 4a shows how well the expansion is converging point-wise to the measured values while Fig. 4b shows how the expansion is converging to both the measured values and interpolated values. Both plots include the line $N = 17$, the degree above which the equi-

anglular and Chebyshev quadrature are no longer exact. The plots reveal many salient trends in relation to the quadrature schemes and the least-squares approximation. As shown in Eq. (15), the error introduced by a quadrature rule can be zero at some degrees but significant at others. For all rules, it is clear that the expansion begins to converge to the sampled values, until at some point the error $E[f]$ becomes substantial. At this point, the error severely impacts the quality of the expansion, as seen by a sharp increase in the RMSD values. This point is typically well beyond the degree of exactness. For example, Simpson's composite 3/8th is capable of integrating piece-wise polynomials of degree $P = 3$, but it begins to deviate from the other methods around spherical harmonic degree $N = 13$ before becoming very inaccurate at degree $N = 20$. The equi-anglular weights are accurate to degree $N = 17$, but error from the quadrature rule becomes substantial around degree $N = 30$ before becoming very problematic at degree $N = 36$. Interestingly, while the modified effective sampling area weights are not exact to any degree, they outperform the equi-angle weights, maintaining stable convergence up to near degree $N = 35$. The Chebyshev weights are exact to degree $N = 17$, the same as the equi-anglular weights. However, their error functional is much smaller; they perform the best of all the tested quadrature rules. Thus, when considering a quadrature scheme, perhaps of greater importance than the degree of exactness is the error functional. This is illustrated by the effective area weights, which are not exact to any degree but outperformed the equi-angle scheme, which is exact to degree $N = 17$. The difficulty lies in the fact that the error function is difficult to derive and is typically only provided for simpler quadrature schemes.

A notable trend occurs with the least-squares approximation. In Fig. 4a, it appears that as the degree increases, in turn adding new columns to the matrix $\mathbf{Y}$ and increasing its span, the error at the sampled points tends to zero. However, from Fig. 4b it is evident that at points in between, the error has not improved and becomes especially significant at degree $N = 44$. Interestingly, when one only looks at the point-wise convergence, one would assume that the best approximation occurs when $N = 45$; however, the overall fit to the underlying function becomes worse than at many lower degrees. This effect is commonly referred to as overfitting and is further illustrated in Fig. 5. Figure 5a shows the least-squares approximation at $N = 45$ on the regular 5° grid, which appears to have converged to the desired function. However, when one looks at interpolated values, as shown in Fig. 5b, it is clear that the expansion deviates from the underlying function. At a lower degree $N = 35$, the interpolated values agree better. Thus, as mentioned earlier, care must be taken with the least-squares method, as point-wise convergence to measured values does not ensure that interpolation between values will be valid. Furthermore, for this sampling scheme with 2,552 points, the recommendation of $(N + 1)^2 < Q$ (see Sec. 4A) corresponds to a maximal degree $N = 49$ expansion; however, this degree would not provide optimal results. With the quadrature methods, the degree at which the convergence to sampled points begins to worsen is roughly where global convergence begins to worsen. With the least-squares method, the apparent optimal degree for convergence at sampled points may have poor global convergence.

This undesirable effect of the least-squares method is further illustrated in Fig. 6, which compares the L^2 and ℓ^2 norms of the expansions. For an isometric transform, Parseval's relation requires that both the L^2 and ℓ^2 norms should be equal, as defined in Eq. (7). For this figure, the L^2 norm of the unit cube was evaluated using the Chebyshev weights, as they proved to be the most accurate of the other methods. As more terms are added, the ℓ^2 norm of the expansion tends to converge to the L^2 norm. For the quadrature methods, it is clear from a comparison of Figs. 4a and 4b that when the error term in the quadrature method causes the expansion to deviate from convergence to the underlying functions, the increase in signal energy in the newly added but error-laden terms causes the ℓ^2 norm to also deviate. Thus, both comparing the function and sequence space norms and looking at convergence to sampled values are useful tools in evaluating the validity of the expansion. For the least-squares method, while the $N = 45$ degree expansion had the best convergence to the 5°sampled points, Fig. 4b clarifies that the least-squares fit was overfitting the sampled points, which is also detected in the sharp increase in the ℓ^2 norm in Fig. 6. Thus, while in practice the knowledge of the underlying sampled function is unknown, by studying the ℓ^2 norm of the least-squares fit

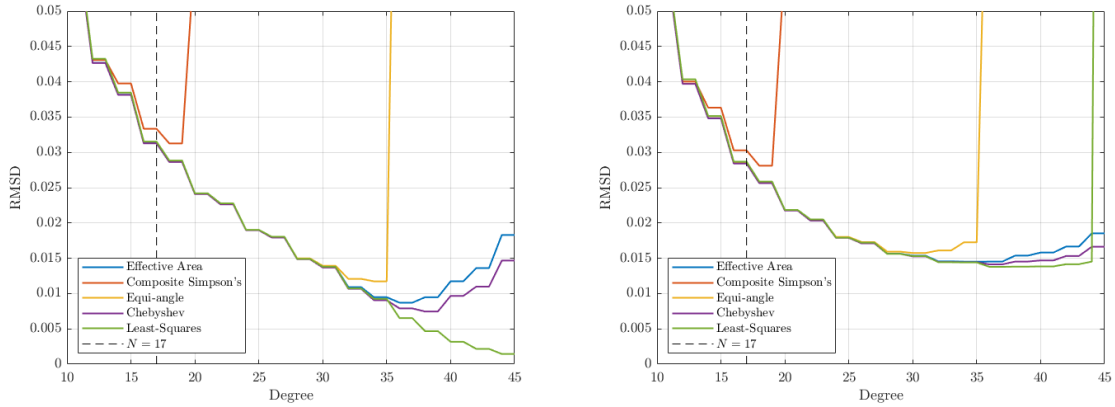

(a) *(b)*

Figure 4: The RMSD between the spherical harmonic expansion over 5° and 2.5° grids, and known values on the grids, plotted over expansion degree. The spherical harmonic expansion used is the same in both 4a and 4b; however, the finer grid used in 4b allows for a check of whether the interpolated values between sampling points remains valid.

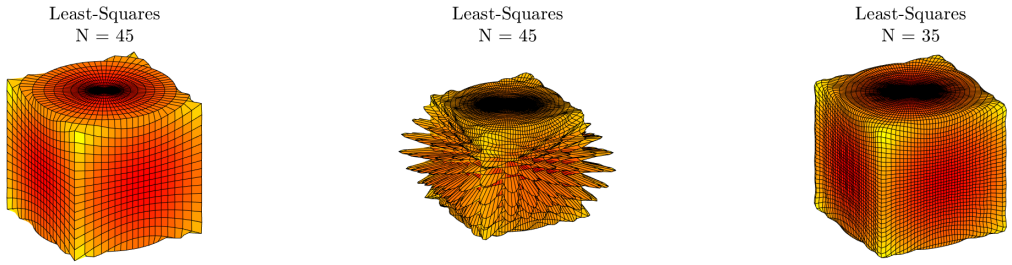

(a) *(b)* *(c)*

Figure 5: Least-Squares spherical harmonic expansion of a unit cube on a 5° and 2.5° grid. (a) The $N = 45$ expansion evaluated on the original 5° grid. (b) The $N = 45$ expansion evaluated on a finer 2.5° grid. (c) The $N = 35$ expansion evaluated on a finer 2.5° grid.

over degree N, one can glean important information as to when the fit is good and when overfitting occurs.

7. SELECTED RESULTS

This section includes figures from musical instruments results. Animated directivity data based on $N = 10$ degree spherical harmonic expansions are available online.[11] Figure 7 shows the directivity balloon of a measured Bassoon at 550 Hz (5th partial of A2) over varying expansion degree. With increasing degree, the interference lobes become more apparent. Figure 8 shows the measured trombone directivity at 490 Hz (5th partial of G2). The balloon shows a vantage from behind the trombone, highlighting the quasi-symmetric diffraction caused from the seated musician and chair, which is also apparent in the corresponding polar plots.

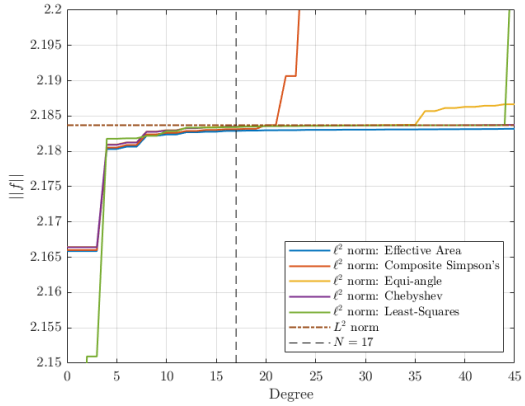

Figure 6: The ℓ^2 norms over degree of expansion of select methods for approximating the unit cube using a spherical harmonic expansion.

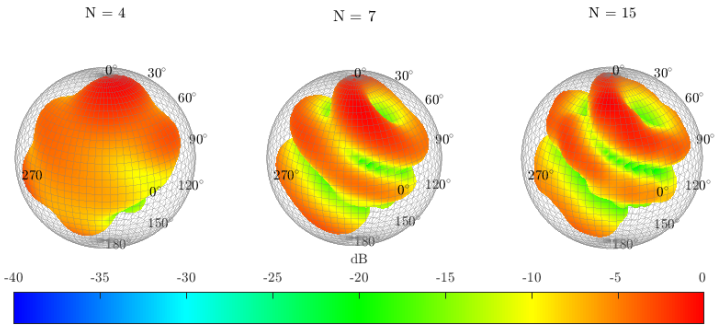

Figure 7: Bassoon directivity balloon at 550 Hz over varying expansion degrees.

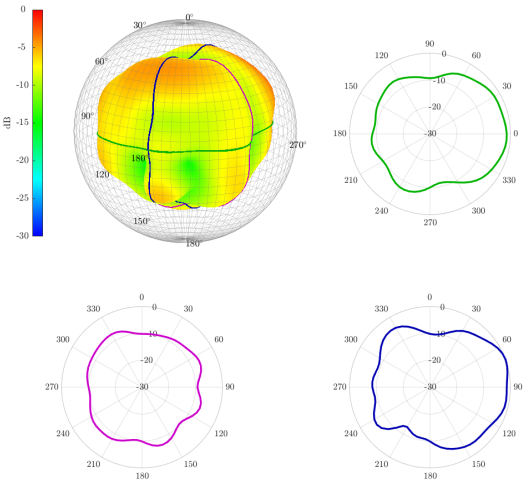

Figure 8: Trombone directivity at 490 Hz. Balloon shown from behind the musician.

8. CONCLUSION

Directivities of live sources, such as musical instruments, are useful for a variety of applications. This work has reviewed various techniques for computing their spherical harmonic expansions and helped to provide further insights. Least-squares approximation and quadrature methods have been compared; both have been shown to be effective at providing meaningful results, provided adequate care is given to ensure optimal expansion. While the least-squares method has the advantage of being applicable to variety of sampling schemes, quadrature rules are useful in that they can be used to compute integrals over the sphere for applications such as evaluating errors in spherical data or computing sound power. Of the quadrature rules examined, the newly presented Chebyshev scheme performed the best for the 5°AES directivity sampling standard. Future work includes studying the necessary sampling degree for musical instruments and expanding applications of spherical harmonics for directivities.

ACKNOWLEDGMENTS

This research was funded in part by the Institute for Scientific Research in Music.

REFERENCES

[1] Bodon, K. Joshua. *Development, Evaluation, and Validation of a High-Resolution Directivity Measurement System for Played Musical Instruments*. Master's Thesis, Brigham Young University, 2016.

[2] *AES Standard on acoustics - Sound source modeling - Loudspeaker polar radiation measurements*. AES56-2008 (r2019), Audio Engineering Society.

[3] Williams, E. G. *Fourier Acoustics*. London Academic Press, 1999.

[4] Rafaely, Boaz. *Fundamentals of Spherical Array Processing*. Springer-Verlag, 2015.

[5] *Common Loudspeaker Format*, Common Loudspeaker Format Group, 2017. http://www.clfgroup.org.

[6] ISO 3745:2012.*"Acoustics – Determination of sound power levels and sound energy levels of noise sources using sound pressure – Precision methods for anechoic rooms and hemianechoic rooms."* International Organization for Standardization, Geneva, 2012.

[7] Leishman, Timothy W., Rollins, Sarah, and Smith, Heather. *An experimental evaluation of regular polyhedra loudspeakers as omnidirectional sources of sound*. Journal of the Acoustical Society of America, vol. 120, no. 3, 1411-1422, 2006.

[8] Davis, P. J., and Rabinowitz, P. *Methods of Numerical Integration*. Academic Press, 1984.

[9] Driscoll, J. R. and Healy, D. M. *Computing Fourier Transforms and Convolutions on the 2-Sphere*. Advances in Applied Mathematics, vol. 15, no. 2, 202-250, 1994.

[10] Mason, John C., and Handscomb, D.C. *Chebyshev Polynomials*. Chapman and Hall/CRC, 2003.

[11] https://scholarsarchive.byu.edu/directivity.